Natural Hazards **24:** 105–131, 2001.

Test of Source-Parameter Inversion of Intensity Data

L. SIROVICH[1], F. PETTENATI[2] and C. CHIARUTTINI[3]
[1]*The National Institute for Oceanography and Experimental Geophysics – OGS, Trieste, Italy, E-mail: sirovich@ogs.trieste.it;* [2]*The National Group for Defence Against Earthquakes (GNDT) of the National Institute for Geophysics (ING), Rome, Italy, at OGS, E-mail: pettenati@ogs.trieste.it;* [3]*Dept. Naval Architecture, Marine and Environmental Science, University of Trieste, Trieste, Italy, E-mail: chiaruttini@univ.trieste.it*

(Received: 28 June 2000; in revised form: 27 October 2000)

Abstract. We demonstrate that the approximate source kinematics of the San Fernando, 1971 earthquake can be back-predicted by analysing its macroseismic intensity data set (felt reports) objectively and quantitatively. This is done by inverting either the data set of the intensity values observed in all sites, or the intensities tessellated with the Voronoi polygons technique. It is shown that the kinematic characteristics found following our method (epicentral coordinates, source depth, seismic moment, rupture length, Mach number, fault plane solution) match those determined by other authors, via instrumental measurements, rather well. The prerequisite for obtaining these results is that local amplification must not affect groups of neighboring sites. It was possible to invert the U.S.G.S. "felt reports" for the source because this data set is sufficiently uncontaminated by local site responses, and retains relevant regional traces of source effects. Isoseismal maps cannot be safely used for this task, because qualitative drawing criteria give subjective results. Isoseismals, based on incomplete space frequency samplings, give rise to spurious effects, whereas the Voronoi polygons produce easy-to-grasp, quantitative and objective, representations of macroseismic intensity data. The tests performed, up to now on a series of earthquakes, suggest that the combined use of tessellation and of our KF model is promising mostly for inverting intensities of preinstrumental earthquakes.

Key words: source inversion, synthetic intensity, Voronoi polygons, tessellation, macroseismic intensity, felt reports, San Fernando earthquake

1. Introduction

One of the earliest concepts which made its way into seismology was the classification of earthquake related damage in terms of the so-called macroseismic intensity, I, observed in the field. It was also thought that the regional I data carry information about its source (e.g., Mallet, 1862; Kövesligethy, 1907; Jànosi, 1907; Blake, 1941; Sponheuer, 1960; Shebalin, 1973; Ohta and Satoh, 1980; Suhadolc *et al.*, 1988; Zahradnik, 1989). Then, Panza *et al.* (1991), Bakun and Wentworth (1997), Gasperini *et al.* (1999) retrieved some source characteristics of earthquakes from I data.

I contains valuable seismological information, and is essential for the study of earthquakes of the preinstrumental era. In a previous paper (Pettenati *et al.*, 1999) we have summarized its strengths and deficiencies; valuable results have recently been obtained, however, after *I* was analysed with new, more quantitative techniques (e.g., Frankel, 1994; Johnston, 1996a,b; Bakun and Wentworth, 1997).

Contouring practices used to produce isoseismals were examined in other papers of ours (Pettenati *et al.*, 1998, 1999). In brief, the data sets of the macroseismic intensity values observed in all sites (in the following: *I* data sets) are the result of the superposition of regional effects (radiation from the source, path) and of local effects (geological and topographical heterogeneities). Strictly speaking, both effects result from continuous phenomena, but at a regional scale local heterogeneities appear to be discontinuous because of the (unavoidably) insufficient sampling provided by the macroseismic surveys. It was stressed that conceiving isoseismal maps as a picture of the global phenomenon, which could overcome the scantiness of available observations, is an ill-posed approach. Due to the non-homogeneous regional distribution of surveyed sites, isoseismals drawn manually or automatically do not often obey the spatial version of the Nyquist principle along the coordinate axes (Press *et al.*, 1994; pp. 494–495). As a consequence, they are often unreliable. In other words, high sampling densities (many surveyed sites) carry detailed information on intensity patterns; but only the tendency of *I* to decrease with epicentral distance (i.e., the low-frequency part of the phenomenon) may be confidently deduced when isoseismals are traced using very few points. Our contribution promotes new objective procedures, suggests overcoming the established practice of tracing isoseismals, and renders inversion of *I* data sets feasible.

We use tessellation with Voronoi polygons (Preparata and Shamos, 1985; Pettenati *et al.*, 1999; Figure 4) for visualizing the earthquakes' effects. Sambridge *et al.* (1995) and Li and Götze (1999) demonstrated the efficiency of this technique in gridding highly irregular distributions of geophysical data, and its usefulness in solving inverse problems. Thus, for inversions, we use traditional statistical tests on residuals of *I* data sets, and of tessellated regional intensities. To invert *I* data for the source we use our kinematic model KF (Chiaruttini and Siro, 1991; Sirovich, 1996b).

In this paper we test the possibility of inverting the "felt reports" received by the United States Geological Survey USGS (kindly provided by J. W. Dewey, 1994, written comm.) to retrieve the epicentral coordinates, source depth, seismic moment, rupture length, Mach number, and fault plane solution of the studied earthquake (see later).

The USGS data are expressed in the Modified Mercalli Scale MM (Wood and Neumann, 1931). Note that, in the case of the San Fernando, 1971 earthquake, the USGS catalog contains one degree XI datum (Sylmar; 34°.308N, 118°.448W), and one degree X (San Fernando; 34°.282N, 118°.438W), and no IX degrees; we reduced these two epicentral data to degree IX, according to Bakun and Wentworth

(1997); thus, degree IX was assumed as the maximum observed intensity $I_{\max}$ of this earthquake. The term "pseudo-intensity", i, is used for the intensity values expressed in real or integer numbers.

Regarding the discontinuous component of I data, the problem of distinguishing singular sites with local amplifications or de-amplifications cannot be overcome in a simple manner. We prefer not to filter the data; rather, we look for outliers using statistical techniques, and then we analyse residuals following a neutral empirical approach (see later on).

We have another purpose as well: to do a statistical test and ascertain if our KF values estimate i at the sites better than what is done for practical purposes using empirical relations of the so-called 'attenuation' (which mix rather different phenomena). If this holds, the synthetic values of pseudo-intensity obtained from our model, in some cases, could usefully substitute the 'attenuation' relations in algorithms which calculate regional seismic hazard.

Finally, it is more than evident that the already available fault-plane solutions of the 1971 San Fernando earthquake are more reliable than ours, because they were obtained based on instrumental measurements, that are much more reliable and easier to treat than felt report data. We wish to see if, by using the intensities, it is possible to get an approximate idea of the source of this earthquake. To expect anything more would be unrealistic. In any case, this would already be a significant result because it would be promising for studying pre-instrumental events: retrieving source information from I data sets would improve the knowledge on hazard in areas with rich historical catalogues and/or low seismicity rates and rare strong earthquakes.

2. Synthetic Intensities

To calculate synthetic pseudo-intensity i from the dimensionless values of KF, given by Equation (1) (Sirovich, 1996a,b; also see Pettenati *et al.*, 1999), we used the data-fitting function) in Equation (2)

$$\mathrm{KF}(P, l) = \frac{R(P, l)}{\Delta_{sr}(P, l)[1 - (Vr/Vs)\cos\theta(P, l)]}. \tag{1}$$

In Equation (1), KF is the contribution of a source point (the rupture propagating along a linear fault at depth H), at a distance l from the nucleation point, to the displacement-related ground motion at the receiver point P on the surface. R is the radiation pattern of S-waves (Aki and Richards, 1980; p. 115), Δ_{sr} is the distance between source-receiver points, Vr is the rupture velocity, Vs is the S-wave velocity, and θ is the angle between the ray reaching P and the direction of the rupture propagation (see the definition of Cartesian coordinates in Sirovich, 1997; Figure 1). Note that the asymptotic assumption (upon which our KF model rests) is satisfactory at distances of the order of the wavelength from the source

Table I. The five earthquakes, that struck the greater Los Angeles area under study.

Earthquake	Date	M_0 (dyne cm)	Reference
San Fernando	Feb. 09, 1971	2.2×10^{26} [a]	Alewine, 1974
Whittier Narrows	Jan. 10, 1987	1.0×10^{25} [b]	Bent and Helmberger, 1989
Upland	Feb. 28, 1990	3.97×10^{24} [c]	CMT catalog, 1994
Sierra Madre	June 28, 1991	2.7×10^{24} [d]	Ma and Kanamori, 1994
Northridge	Jan. 17, 1994	1.5×10^{26} [e]	Song *et al.*, 1995

[a] Estimated from static displacements.
[b] From modeling of long- and short-period body wave form data recorded at regional and teleseismic distances.
[c] From centroid-moment tensor inversion.
[d] From combining the wave form and first-motion data of high-quality broad band and wide dynamic range TERRAscope seismograms.
[e] From modeling broad band regional records using empirical Green's functions (value at the upper limit).

(Madariaga and Bernard, 1985; Bernard and Madariaga, 1984; Spudich and Frazer, 1984); then, at 80–100 km beyond it, surface waves prevail.

$$\begin{aligned} \mathrm{i}(x, y) \;=\; & 118.488 - 9.686 \cdot \log M_0 + 0.215 \cdot (\log M_0)^2 + (-0.946 \\ & +0.258 \cdot \log M_0) \cdot \log \mathrm{KF}(x, y) + 0.810 \cdot (\log KF(x, y))^2. \end{aligned} \quad (2)$$

In Equation (2), $\mathrm{i}(x, y)$ is pseudo-intensity at location (x, y), $\mathrm{KF}(x, y) = \max_l \mathrm{KF}(P, l)$ is referred to a Cartesian plane, and M_0 is the seismic moment in dyne cm. This data-fitting function was adapted to 1720 I data of the five earthquakes of the greater Los Angeles region, listed in Table I; thus, it holds within IV $\leq$ I $\leq$ IX, $2.7 \times 10^{24} \leq M_0 \leq 2.2 \times 10^{26}$ dyne cm, and $-3.260 \leq \log \mathrm{KF} \leq -0.108$. We chose data from shocks in the same area to minimize the effects of the crustal- and site-structures.

To translate KF values into i, we used linear regressions first (Sirovich *et al.*, 1998), but then adopted the polynomial model of Equation (2). In so doing, the overall improvement of the fits is small, but we made this choice because, in using the linear model, the highest residuals (calculated-minus-observed) are concentrated in the range of the highest intensities, and we wanted the best fit for them. Pseudo-intensity i is taken as an integer number; given the nature of intensity (which is expressed in a discrete and bounded scale on a qualitative basis), the real numbers produced by Equation (2) were rounded to integers by truncation. The seismic moments used (which optimize the model of Equation (2)) are listed in Table I; the ANOVA test shows that the overall quality of the model is good; in fact, the probability of the null hypothesis is $< 10^{-5}$.

Figure 1 summarizes how Equation (2) works with the five earthquakes which were used to calculate the fitting function. Note that in the figure the mean values

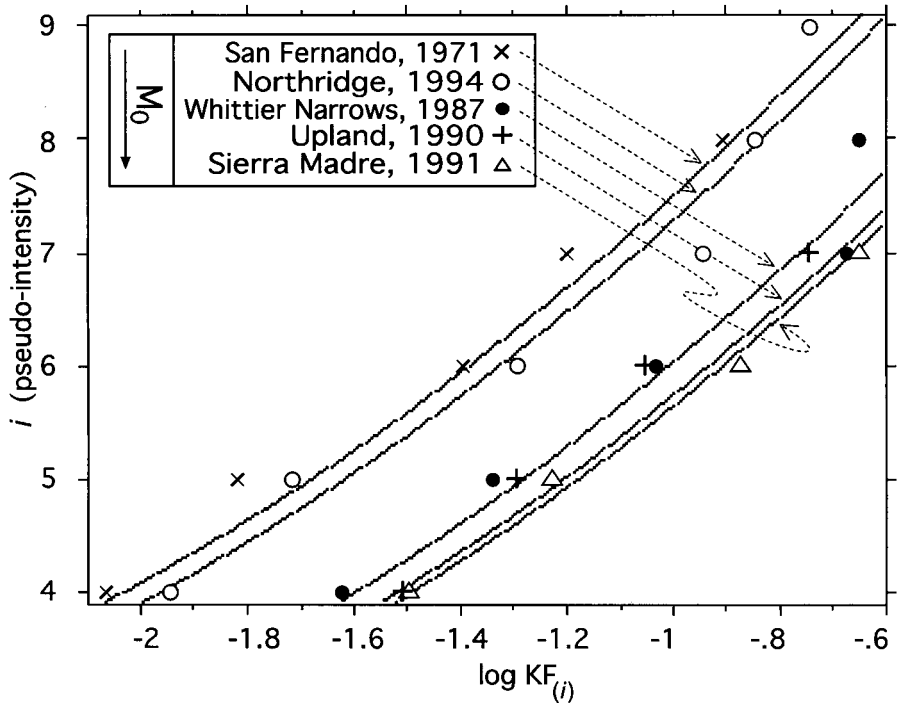

Figure 1. Pseudo-intensity i versus mean values of log KF(i) for the five earthquakes studied.

of log KF(i) for the strongest shocks (San Fernando, and Northridge) are clearly separated from those of the smallest ones (Upland, and Sierra Madre), with the data of the intermediate $M = 1.0 \times 10^{25}$ dyne cm Whittier Narrows earthquake (Bent and Helmberger, 1989) lying approximately in between. This led us to include more variables in the (log KF; i) regressions so as to take into overall account the 'size' of the earthquakes; the seismic moment fitted this purpose.

Before calculating function (2), we removed the outliers from the I data set. The search of outliers gave us the opportunity of making some observations about local site responses.

3. Outliers and Site Effects

Given the log-normal statistical model, the classic Chauvenet method (Barnett and Lewis, 1978; pp. 19–20; also see Johnston, 1996a) was applied. As a whole, out of the five earthquake sets, sixteen outliers over 1720 sites were found in this way, plus three questionable data (Overton, Sylmar, Bullhead City). However, since the three aforementioned data were clear outliers in the Gamma distribution, according to the «discordancy test» (Barnett and Lewis, 1978; pp. 79–81), they were cut out of the data set used. The resulting nineteen outliers are listed in Table II; distances D and a gross soil classification are also shown there. The classification

Table II. List of outliers.

Earthquake/ Name of station	*D* (km)	*I*	Response	Soil type[a]
San Fernando, Feb. 09, 1971				
Overton	429	4	+	Unknown
Acton	20	5	−	Unknown
University City	208	6	+	Weak rock/stiff soil
Wheeler Ridge	513	5	+	Unknown
Whittier Narrows, Jan. 10, 1987				
Sylmar	252	5	+	Unknown
South San Gabriel	6	6	−	Weak rock/stiff soil
Upland, Feb. 28, 1990				
Cucamonga	10	4	−	Soft soil
Guasti	13	4	−	Soft soil
Goleta	199	5	+	Soft soil
Alta Loma	3	5	−	Soft soil
Sierra Madre, June 28, 1991				
Santa Clarita	14	4	−	Rock
Salton City	218	4	+	Weak rock/stiff soil
Palm Desert	160	5	+	Weak rock/stiff soil
Mount Wilson	7	6	−	Rock
Northridge, Jan. 17, 1994				
Saugus	22	4	−	Soft soil
Los Nietos	51	4	−	Soft soil
Glendora	63	4	−	Soft soil
Bullhead City	379	5	+	Unknown
Reseda	1	8	−	Soft soil

[a] Data by R.M.S. Inc., Fouad Bendimerad (1997, written comm.).

of the prevailing soil at each site comes from the Geographical Information System, G.I.S., of Risk Management Solutions Inc., R.M.S., and was furnished by Fouad Bendimerad (1997, written comm.). The classification used by R.M.S. is as follows (R.M.S. lists also "artificial fill/bay mud", and "unknown").

Class 1 (rock): Hard to firm rock, mostly metamorphic and igneous; fresh conglomerates, sandstones and shales without intensive fracturing. Shear wave velocities generally >700 m/s.

Class 2 (weak rock/stiff soil): Gravelly soils to weak rock. Deeply weathered and highly fractured bedrock. Soils with more than 20% gravel. Alluvial cover less than 5–10 m thick and not water-saturated. Shear wave velocities 375–700 m/s.

Class 3 (soft soil): Stiff clay and sandy soils. Loose to dense sands, silty or sandy loams, and medium to stiff/hard clays. Water-saturated alluvial deposits. Holocene alluvium >10 m thick. Shear wave velocities 200–375 m/s.

Note that most sites were repeatedly damaged by the five earthquakes studied, but none of them are mentioned twice in Table II. Therefore, it seems that systematic, strongly anomalous, amplifications or deamplifications might be excluded *from the statistical point of view*. The responses of sites in the Salton Sea Basin area are worth commenting on, however, from the point of view of *physical* amplification. Statistics indicate only Palm Desert ($I = 5$) and Salton City ($I = 4$) as outliers (during the Sierra Madre event). (Both are classified "weak rock/stiff soil" by the G.I.S. prepared by R.M.S. Inc.). But almost systematic positive response anomalies were found in the area during the two strongest earthquakes (San Fernando, 1971 and Northridge, 1994) among the five studied. In these two I data sets, positive anomalies depict a NW-SE trough that approximately matches the wide stripe of rather soft sediments which is found in the Basin area. The Palm Desert, Indio, and Quinta sites (all soft soils) performed a physical amplification during the Upland earthquake as well. In their vicinity, Thousand Palm, Cathedral City, and Rancho Mirage (all on soft soil) showed a moderate amplification also during the Whittier Narrows shock. The presence of a positive anomaly during the Northridge, 1994 earthquake, in the vicinity of the Salton Sea Trough, is also detected by Dengler and Dewey (1998).

Table II also shows that both sites, which gave statistically anomalous low I values during the relatively small earthquake of Sierra Madre, are rather close to the source and are on rock. On the contrary, for the Upland earthquake, which had a magnitude close to that of the Sierra Madre, all statistically anomalous deamplifications pertained to sites on soft soil, close to the source. From this rapid overview, it is evident that Table II does not lead to simple suggestions about soil-distance-magnitude-amplification relationships.

Before performing the inversions, we searched for site effects on damage. We did this by splitting the $\log D(I)$ data of the samples of each earthquake according to the soil prevailing at each site (the aforementioned three classes by R.M.S., Fouad Bendimerad, 1997, written comm.). From the statistical point of view, we did not find systematic anomalous amplifications or deamplifications. As examples, Tables III and IV show the descriptive statistics of the split samples of the two strongest earthquakes (the count of scanty data are in bold). It is seen that, for a certain I degree, the differences between the mean values of $\log D$, as a function of soil type, are generally less than one standard deviation. The mean values of $\log D(I = \text{VII})$ of the San Fernando event are the only exceptions. In this case, there is a tendency for Class 3 (soft soils) to 'damp' damage more than Class 2 (weak rock/stiff soil) (there were no sites of Class 1, rock). (The descriptive statistics of the Upland, Sierra Madre, and Whittier Narrows earthquakes are not shown). This finding will be commented on in the Discussion.

Table III. Descriptive statistics of the I data from the San Fernando, 1971 earthquake.

Intensity I	Soil type	Mean log $D(I)$	Std. dev.	Count
IV	1	2.353	0.094	25
IV	2	2.315	0.091	11
IV	3	2.372	0.107	43
V	1	2.147	0.197	26
V	2	2.067	0.194	70
V	3	2.103	0.223	146
VI	1	1.732	0.250	7
VI	2	1.823	0.142	19
VI	3	1.760	0.164	62
VII	2	1.620	0.046	6
VII	3	1.483	0.097	25
VIII	3	1.213	0.137	4

Table IV. Descriptive statistics of the I data from the Northridge, 1994 earthquake.

Intensity I	Soil type[a]	Mean log $D(I)$	Std. dev.	Count
IV	1	2.285	0.110	20
	2	2.221	0.116	33
	3	2.317	0.121	57
V	1	2.068	0.173	23
	2	2.016	0.193	40
	3	2.035	0.226	110
VI	1	1.762	0.153	**3**
	2	1.671	0.099	17
	3	1.656	0.163	33
VII	1	1.218	0.104	**2**
	2	1.291	0.054	**2**
	3	1.353	0.193	20
VIII	1	1.160	0.220	**2**
	2	1.385	0.153	4
	3	1.105	0.248	18
IX	1	1.150	0.144	**3**
	3	0.905	0.337	6

[a] 1=; 2=; 3=. data by R.M.S. Inc., Fouad Bendimerad (1997, written comm.).

4. Inversion of Intensity Data Sets

Our purpose was to tune inversions objectively. From this point of view, we realized that (i) isoseismals are not suitable for this task; (ii) the I data sets are suitable.

Using the I data set, the result of the statistical tests is simply the sum of the squared residuals, or the χ^2, at all sites. In general, we use squared residuals to emphasize residuals >1. In this regard, we stress that an uncertainty of one degree in the I estimate is common in the field. Subsequently, we consider a random geographical distribution of one degree discrepancies between synthetics and observations not determinant. The same does not hold in case of systematic one degree discrepancies in a certain region. Unfortunately, traditional statistical tests upon residuals can estimate the overall quality of the fits, but are unable to study the distribution of residuals geographically. In a previous paper, we proposed to do this quantitatively and objectively, by computing statistical tests in the tessellated plane (Pettenati et al., 1999).

To consider the geographical distribution of residuals, we perform two different tests. Test «V-V» (V stands for Voronoi) involves the following steps: (i) the plane is tessellated and the residual calculated at each site; (ii) each squared site residual is weighted with the inverse of the area of the polygon, W_p, where the site is located; (iii) the sum of all weighted squared residuals is performed (see Table VI). Test «C-V» («Continuous over Voronoi»), is as follows: (i) the calculated function is sampled on a regular grid with an elemental area dS, these samples are then compared with the corresponding values of the tessellated observations (see Figure 2); (ii) the weighted residual $(\mathrm{cal_i} - \mathrm{obs_{i'}})$ is calculated for each element dS (w_i) rewards small polygons, and penalizes elemental areas close to the borders of the largest polygons; see details in Pettenati et al., 1999); (iii) the sum of the weighted squares is computed over the whole area of the figure. Visually, the result of the C-V test is the distribution of the residuals which is delimited by the intersection between the synthetic radiation (curves) and the tessellated observations (see Figures 6, 8, and 11). Both V-V and C-V tests give low importance to squared residuals obtained from isolated sites (i.e., large polygons, usually far from the source).

Residuals are also divided into classes of intensity; and we even check which percentage of the total (tessellated) area of a certain intensity degree is correctly forecast by our kinematic model. Concentrations of residuals (positive and negative) can be easily visualized on a tessellated plane (see Figures 5 and 11).

Consider that we started our experiments without knowing the shape of the Σr^2 surface of this new kind of intensity inversion. Thus, we could not use available automatic inversion algorithms, which speed the inversion, but could converge towards a relative minimum. Rather, we decided to put some instrumental constraints on the parameters searched and find the minimum variance model within these constraints. See later, the constraints used for the San Fernando earthquake.

Conservatively, we quantified the errors of the principal parameters obtained from inversion, assuming that an error of two degrees in the I estimate is unlikely.

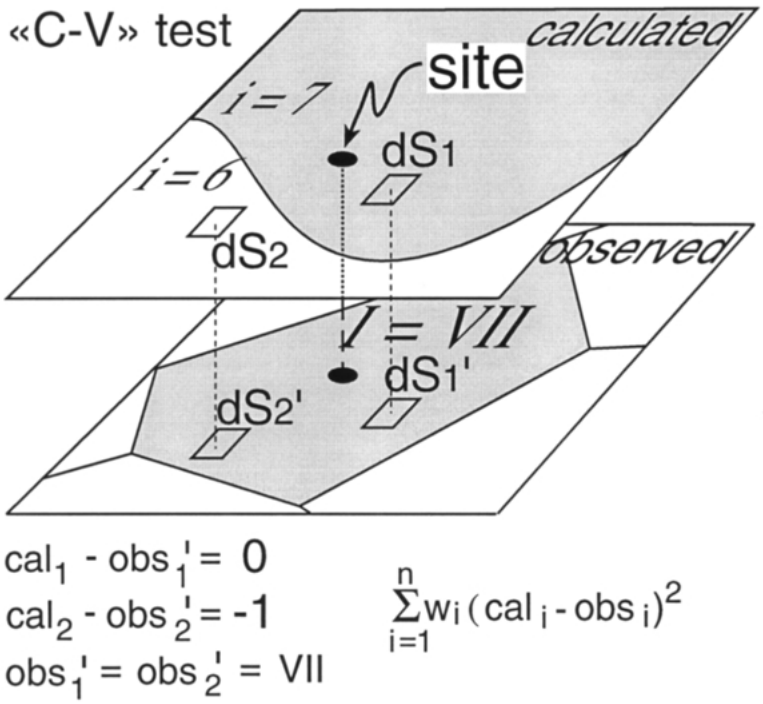

Figure 2. Definition of the C-V residual test (see text).

So, we progressively increased (and decreased) the parameters of the best fitted solution, one by one, by trial-and-error, till the first site experienced an i change of two degrees (see the procedural details in Sirovich and Pettenati, 1999). These errors are conservative because the allowed variation for each single parameter results in at least one site to change by the maximal assumed uncertainty of the I estimates. The asymmetry of the calculated errors in Table V is due both to the incomplete sampling provided by the sites, and the functional expression of Equation (2); note that the reliability of these errors deteriorates at the extremes of the validity of Equation (2).

We followed this approach to repeat the inversion of the I data set of the San Fernando, 1971 earthquake, already treated some years ago (Sirovich, 1996a). In that paper, synthetic and 'observed' isoseismals were compared qualitatively. The kinematic characteristics presented in this study (see Table V) were obtained from inversion using the V-V test; the residuals of the C-V tests, and of the I data set, are shown for comparison. The C-V test also enlightens some other consequences of the incomplete sampling of I provided by the surveyed sites (see later).

Table V. Kinematic characteristics of the San Fernando, California, earthquake of 3 February 1971, obtained from inversion of macroseismic intensity.

Parameter Reference	Latitude, longitude (°)	Hypo. depth, H (km)	Strike angle (°)	Dip angle (°)	Rake angle (°)	S-wave velocity, Vs (km/s)	Rupture velocity, Vr (km/s)	Linear rupture, L (km)
This study	34°37′N 118°42′W	13 (+7 −5)	295 (+8 −6)	55 (+11 −18)	90 (+10 −7)	3.5	2.10	20[a]
Sirovich (1996a)	34°26′N 118°41′W	13	290	58	81	3.5	2.45	28[b]

[a] 5 km along strike; 15 km anti-strike.
[b] 5 km along strike; 23 km anti-strike.

4.1. THE SAN FERNANDO, 1971 EARTHQUAKE

The isoseismals of this earthquake are in Stover and Coffman (1993; p. 160). Figure 3 shows the observed intensities (courtesy of J. W. Dewey, written comm., 1994) and the tessellation with Voronoi polygons; the scarcity of information north of the San Fernando and Sylmar sites (the black polygons in Figure 3) partly explains the abrupt passage from intensity VIII to VI (and even from IX to VI towards NNE), but an asymmetry of the observed field has also to be taken into account within 30-40 km from the source. After the previous analysis on the influence of site effects, this asymmetry calls to mind source effects. The tessellation of Figure 3 helps to define objectively the intensity continuity and anomalies.

Figure 3 also shows: the two principal segments of the surface fault rupture (in black and white; redrawn from Kamb *et al.*, 1971, and from the U.S. Geological Survey Staff, 1971); the approximate distribution of the aftershocks between 10–15 February 1971 (closed curve; Scholz, 1971); the epicenter best fitting the syntheses of Figure 4 (34°.37, −118°.42: the circle enclosed in a white square); and the conventional epicenter of Sirovich (1996a; 34°.26, −118°.41: an ×). Other epicenters are: Allen *et al.* (1971) (34°.40, −118°.39; instrumental); Hanks (1974) (34°.45, −118°.40 hypocentral depth H = 13 km; instrumental); Heaton (1982; from a two-fault model): 34°.44, −118°.41, with H = 13 km for the lower fault segment; 34°.42, −118°.33, H = 13 km for the upper segment (virtual hypocenter).

By adopting the aforementioned treatment of residuals in the tessellated plane, we inverted the intensity information of Figure 3, and obtained the kinematic characteristics listed in Table V. The synthesis produced by the model in Table V is in Figure 4 (the small obliquely dashed polygon, on the right of the figure, is of III degree). The inversion pointed to $M_0 = 2.60 \times 10^{26}(-3.18 \times 10^{26})$ dyne cm, which corresponds to a Moment Magnitude M = 6.9, with a 0.4–0.5 uncertainty, in accordance to formula $M = 2/3(\log M_0) - 10.7$ in Stover and Coffman (1993; Equation (6)) (we only show the negative error of M_0 because the positive one is beyond the validity of Equation (2)). During inversion, every parameter could vary within rather wide ranges around the values determined by other authors (see

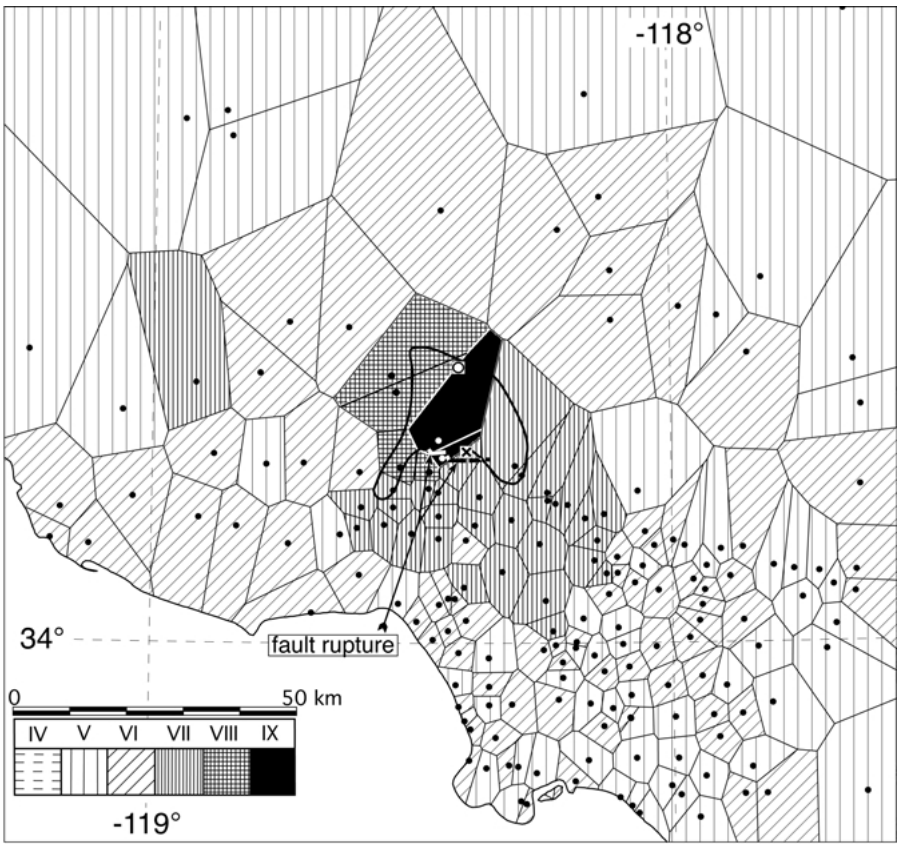

Figure 3. San Fernando, 3 February 1971 earthquake. Observed intensity 'points' (courtesy of J. W. Dewey, written comm., 1994) and tessellation with Voronoi polygons. The surface break of the fault (thick segments; redrawn from Kamb *et al.*, 1971, and U.S. Geological Survey Staff, 1971), and the approximate distribution of aftershocks between 10 and 15 February 1971 (closed curve; Scholz, 1971) are shown. (For the epicenters, see the text.)

these values in Table 1 of Sirovich, 1996a) via instrumental measurements, or via models based on them. These ranges where $\pm 20°$ in strike, $\pm 25°$ in dip, $\pm 35°$ in rake, ± 10 km in rupture length, ± 0.2 in Mach No., ± 5 km in depth, $+0.2$ km/s and -0.5 km/s for Vs, and a radius of 10 km for the position of the epicenter, approximately.

Table V also summarizes the kinematic characteristics determined in 1996. Note that now we are able to propose an hypocenter which is compatible with the positions of the fault break and of the aftershocks (Figure 3), and close to the quoted instrumental determinations. Referring to the 1996 results, the dip angle now matches that measured by Bonilla *et al.* (1971) and by Whitcomb *et al.* (1973). Rupture velocity is lower, but still within the range of values given by Langston in 1978 (1.8 km/s) and by Heaton in 1982 (2.8 km/s).

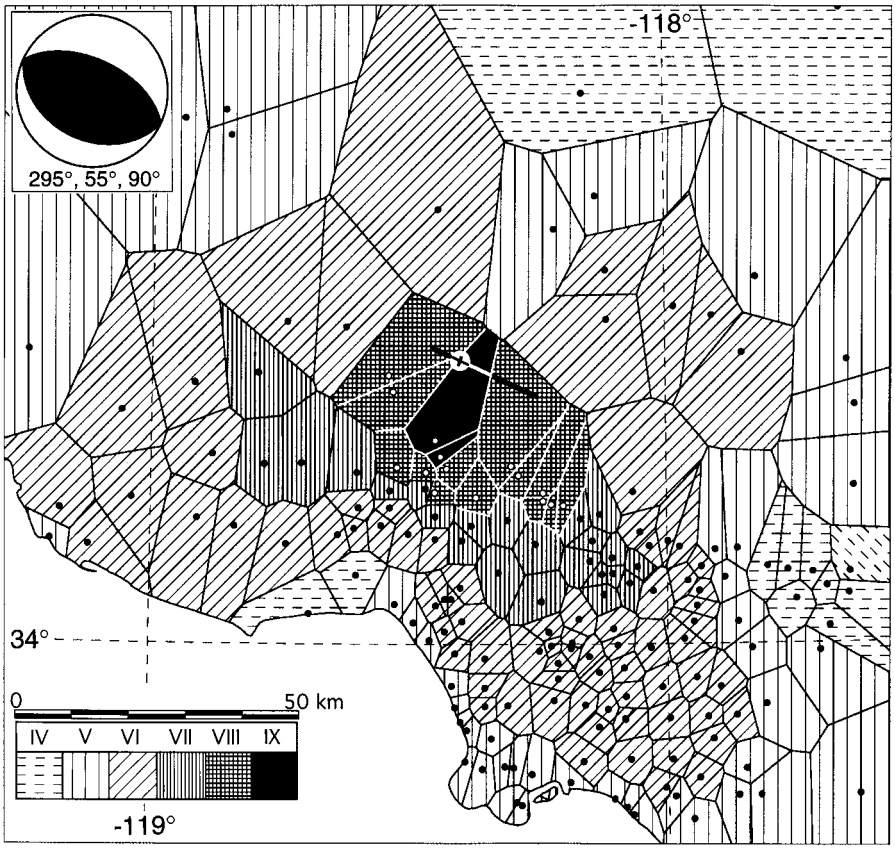

Figure 4. San Fernando, 1971 earthquake. Our best synthetic pseudo-intensities i after tessellation with Voronoi polygons (see the kinematic characteristics in Table V). The fault plane solution, and the line-source with its asymmetric nucleation are also shown.

The syntheses obtained by comparing isoseismals (Sirovich, 1996a) did not allow the quantitative treatment of residuals, and were biased by the spurious information created by contouring in areas not well sampled; consequently, in this particular case, the use of isoseismals masked the result of the survey and rendered the contoured I information less asymmetric than in the I data set obtained from the survey. This conditioned the determination of the length, geometry, and rupture velocity of our linear source in 1996; the problem of the epicenter will be dealt with in the Discussion.

The V-V residuals test (calculated-minus-observed) of our best synthesis of Figure 4 is in Figure 5 and Table VI. Note that there are only six sites (polygons) with absolute residuals $|r| > 1$. The C-V test is in Figure 6; this figure helps explain the cause of the few $|r| > 1$ in Figure 5. At first glance, the cause seems to be the unrealistic prevalence of radiation patterns beyond, approximately, 60 km from the source, but another possibility is hypothesized in the Discussion.

Table VI. Tests on the residuals (San Fernando, 1971 earthquake) in the tessellated plane, and in the *I* data set.

Test	V-V test [:1000] $\sum_{p=1}^{n}(cal_p - obs_p)^2 \cdot W_p$	C-V test $\sum_{i=1}^{n}(cal_i - obs_i)^2 \cdot w_i$	χ^2 V-V test	χ^2 C-V test	*I* data set $\sum_{p=1}^{n}(cal_p - obs_p)^2$	χ^2 *I* data set
Model WHI71	211.3	185,749	0.178	0.192	126	0.127
Our best	154.7	139,084	0.088	0.150	106	0.103

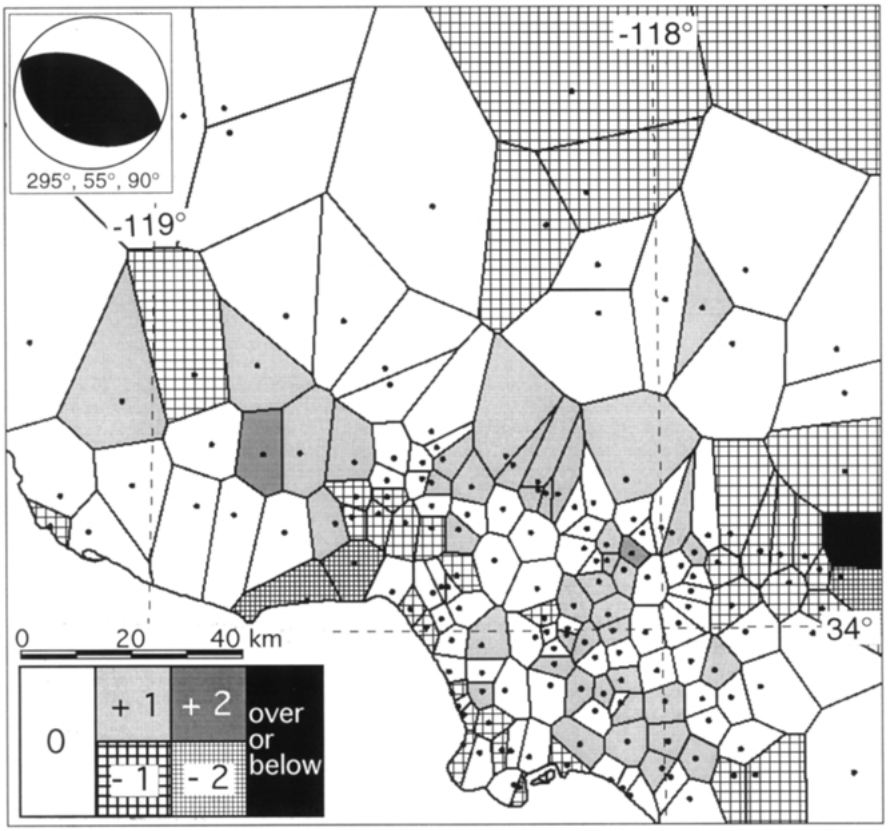

Figure 5. San Fernando, 1971 earthquake. Tessellated intensity residuals of our best synthesis: calculated (Figure 4) minus observed (Figure 3). V-V calculation (see text).

In Figure 7 we show an example of an intermediate step of our trial-and-error inversion test (the obliquely dashed polygon in the upper right corner of the figure is of III degree). This figure was obtained with model WHI71, which adopts the focal mechanism and the 14 km hypocentral depth by Whitcomb (1971), and the following parameters: 34°.44, 118°.41 epicentral coordinates (from model NORMA163 by Heaton, 1982), 5 km along strike and 23 km anti-strike ruptures (Heaton, 1982), 0.7 Mach No., 3.5 km/s for Vs. The major difference between these parameters and those used in Figure 4 is in the value of the angle of rake (64° and 90°, respectively); the comparison between Figures 4 and 7, between Figures 6 and 8, and the inspection of Tables VI and VII highlight the high influence of the rake angle. Figure 8 can be compared with the previous synthesis of Figure 4 in Sirovich (1996a). Note the clustering of positive and negative residuals greater than ± 1 in Figure 8, compared to the more random aspect of Figure 6. The visual comparison between the two V-V tests (not shown here) is even more impressive.

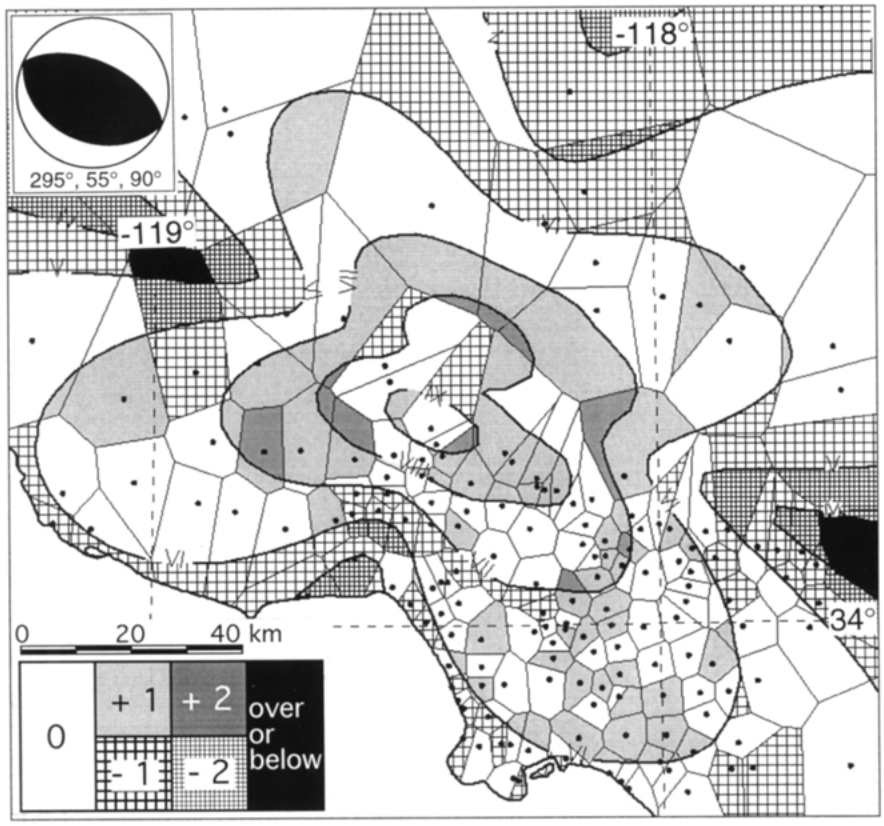

Figure 6. San Fernando, 1971 earthquake. Tessellated intensity residuals of our best synthesis: calculated on a regular grid minus observed (Figure 3). C-V calculation (see text).

Table VII shows: (i) the percentage of the tessellated area of the observed intensity which is correctly forecast by each model, A_{cf}; and (ii) the percentage of the area, A_{nm}, of a given calculated i which does not match (i.e., is outside) the tessellated observations. The ideal synthesis ought to score $A_{cf} = 100\%$ and $A_{nm} = 0\%$. The information in Table VII comes from the comparison between tessellated observations and tessellated calculations (V-V case), and is related to intensities from IX to V. In the A_{cf} field of the table, we also show (in parentheses) the check of the effectiveness of the models by means of the sum of the squared residuals of the sites.

Table VII shows, for example, that our model is able to forecast, correctly, 100% of the area of IX degree (with no errors: $A_{nm} = 0\%$), and 100% of the area of VIII degree; in this case, there is an areal overestimation of 58.9%, which is due to the strong asymmetry of the observed VIII degrees. The comparison between Figures 3 and 4 shows, however, that the overestimation happens above all towards SE and is, only, of one degree. The aforementioned WHI71 model scores an $A_{cf(\mathrm{VII})}$ better than ours, but fails completely to forecast the VIII and IX degrees; note its $A_{nm(\mathrm{VII})}$

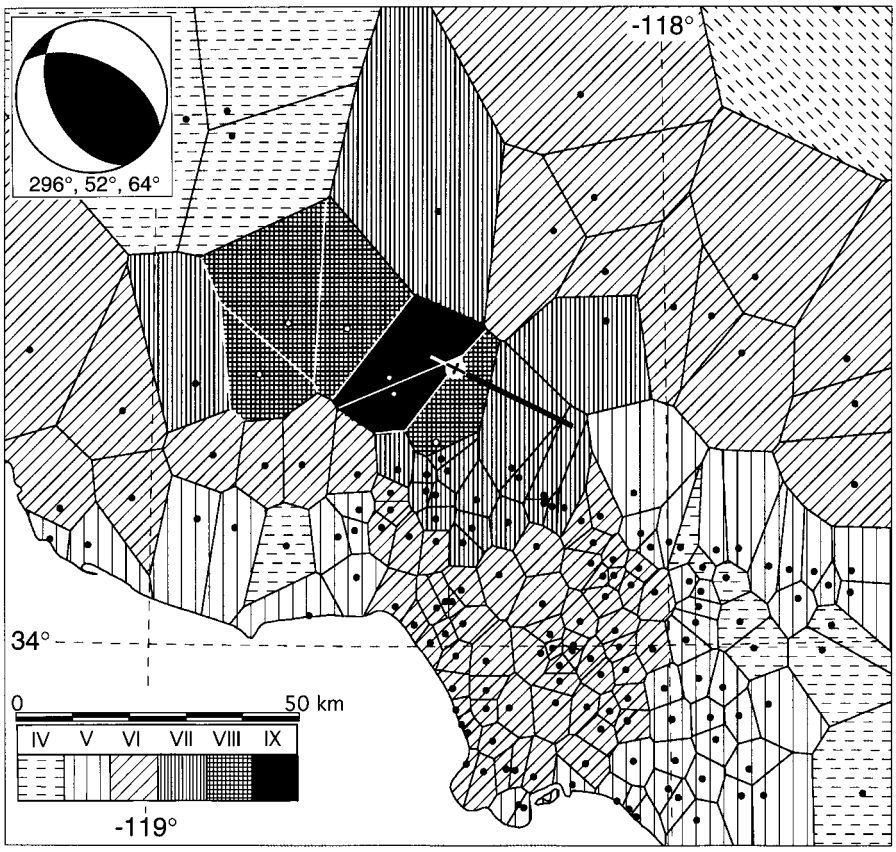

Figure 7. San Fernando, 1971 earthquake. Synthesis obtained using the focal mechanism by Whitcomb, 1971 (model WHI71, see text). Compare with Figure 4.

Table VII. Area- (and point-)check of the effectiveness of two models; (the sum of the squared residuals of the data set of the macroseismic intensity values observed in all sites is in parentheses).

Test / Reference	A_{cf} (%); and ($\sum_{i=1}^{n}$ (cal$_i$ − obs$_i$)^2, I data set)					A_{nm} (%)				
I class	V	VI	VII	VIII	IX	V	VI	VII	VIII	IX
Model WHI71	14.1	44.3	65.6	0.0	0.0	55.9	57.7	60.0	100	100
	(41)	(53)	(23)	(4)	(5)					
Our best model	59.0	66.9	28.9	100.0	100.0	23.6	28.9	57.7	58.9	0.0
	(41)	(47)	(18)	(0)	(0)					

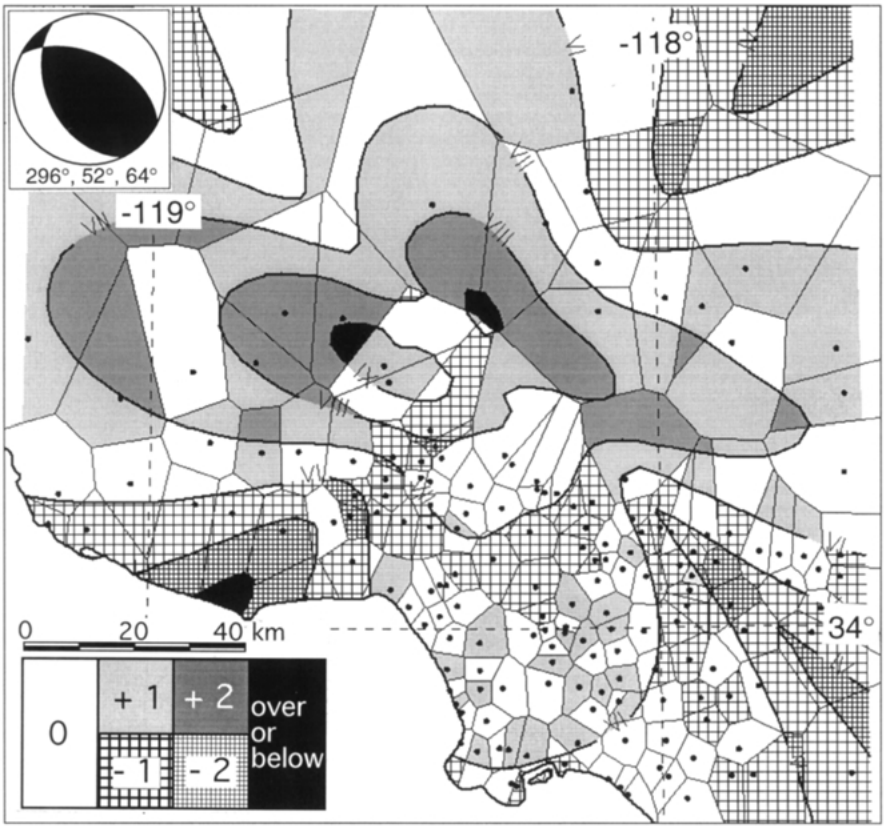

Figure 8. Tessellated intensity residuals of the synthesis of Figure 7 minus observed (Figure 3). C-V calculation (compare with Figure 6, and see text).

= 60.0% (slightly higher than our 57.7%). Also note in the table the sums of the squared residuals of the I data set, which are always in favour of our model, the V degree excepted (for which the two models are equal: 41 against 41).

4.2. FORECAST BY AN 'ATTENUATION' RELATION

We back-predicted the pseudo-intensities of the San Fernando earthquake, according to the established practice of isotropic 'attenuation' relations ($i_{max} - i$; $\log D$) as well. To best predict the i values at the sites, we calculated a new relation using the I data from IX to IV of the five earthquakes studied, emended from the outliers (see Figure 9); for all practical purposes this relation coincides with the well known Blake (1941) model. The term pseudo-intensity is adopted in the figure for the intensity decay forced in a Cartesian axis too.

Figure 10 shows the tessellated pseudo-intensities forecast by the 'attenuation' relation of Figure 9 from the epicenter by Hanks (1974; 34°27′, −118°24′; the

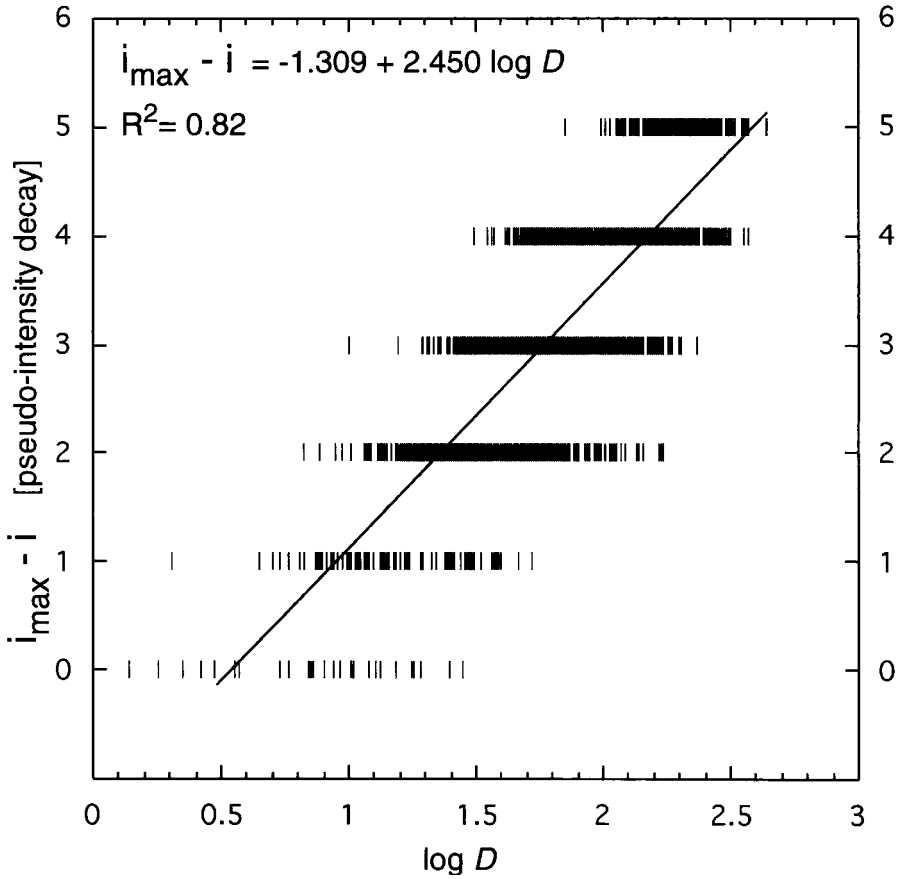

Figure 9. Isotropic 'attenuation' relation for the five earthquake data set (intensity from IX to IV).

cross inside the white dot). In the figure, the intensities of the San Fernando and Sylmar sites (black polygons in Figure 3) are underestimated by at least two intensity degrees (as said, the felt reports of USGS gave I = XI and X there). The asymmetric aspect of Figure 10 is due to the scantiness of the reference sites. No polygons (sites) of degree VIII and IX are back-predicted in Figure 10, but the forecast of degree VI is remarkable. This 'attenuation' relation scores 163.4×10^{-3} in the V-V test (slightly worse than the 154.7×10^{-3} score of our model, and better than the 211.3×10^{-3} score of the WHI71 model using the fault-plane solution by Whitcomb, 1971, in Table VI). The 'attenuation' relation scores a sum of squared residuals, at all sites, of 98, and $\chi^2 = 0.101$, which are slightly better than our model in Table VI (106 and 0.103 respectively); see Figure 11 for relevant details. This figure presents the values forecast by the relation in Figure 9 in every cell dS, minus the observed tessellated intensities of Figure 3 (i.e., the C-V test mentioned; see Figure 2 too). It is shown that the great majority of negative resid-

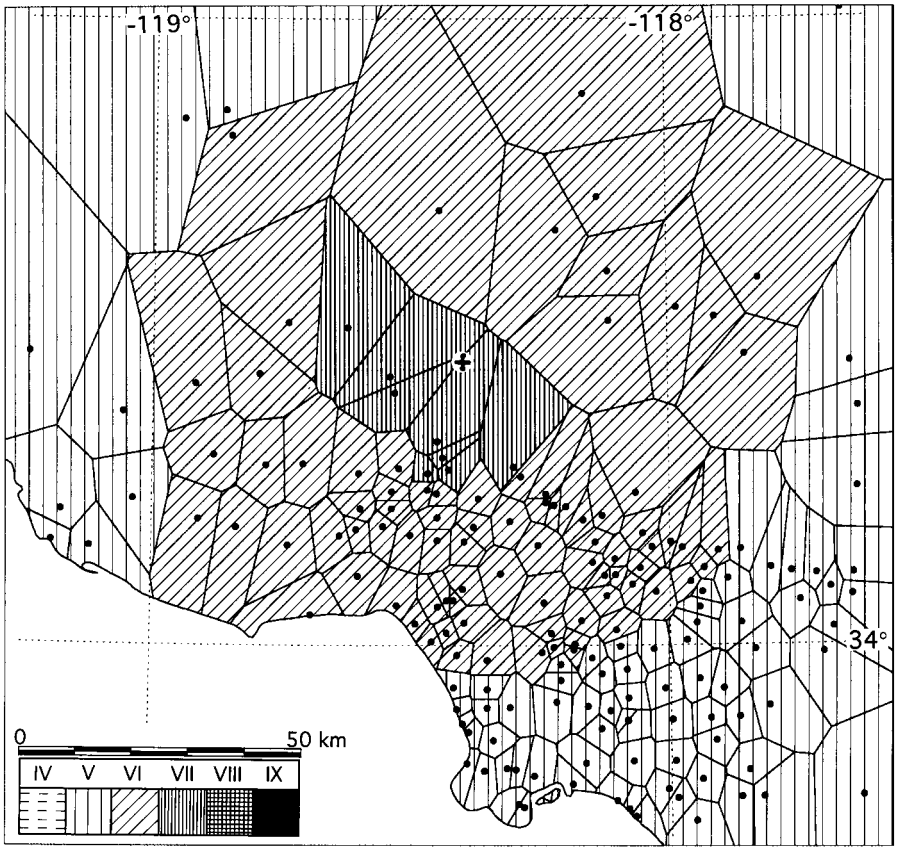

Figure 10. San Fernando, 1971 earthquake. Pseudo-intensities forecast by the 'attenuation' relation of Figure 9 after tessellation with Voronoi polygons.

uals in Figure 11 is found in the lower part of the figure (from WSW to SE), whilst the positive residuals are in the upper part. This means that there is a systematic azimuth-dependent deviation of the forecast from the observed I data set.

5. Discussion

Apart from some cases, such as the sites within the Salton Sea Basin, we did not find any systematic, statistically relevant, dependence of the USGS felt reports from the simplified soil conditions of the sites, in the I data sets of the five earthquakes studied. Note that for the San Fernando earthquake, Boore *et al.* (1978, p. 17) found that "apparently, peak horizontal acceleration is nearly the same, on the average, on rock and soil sites, whereas both peak velocity and displacement are larger on soil sites". We will not speculate here on the more general problem of how strong motion parameters depend on site conditions. We only stress that they are measured very locally, whilst the behaviour of a single edifice is swamped in

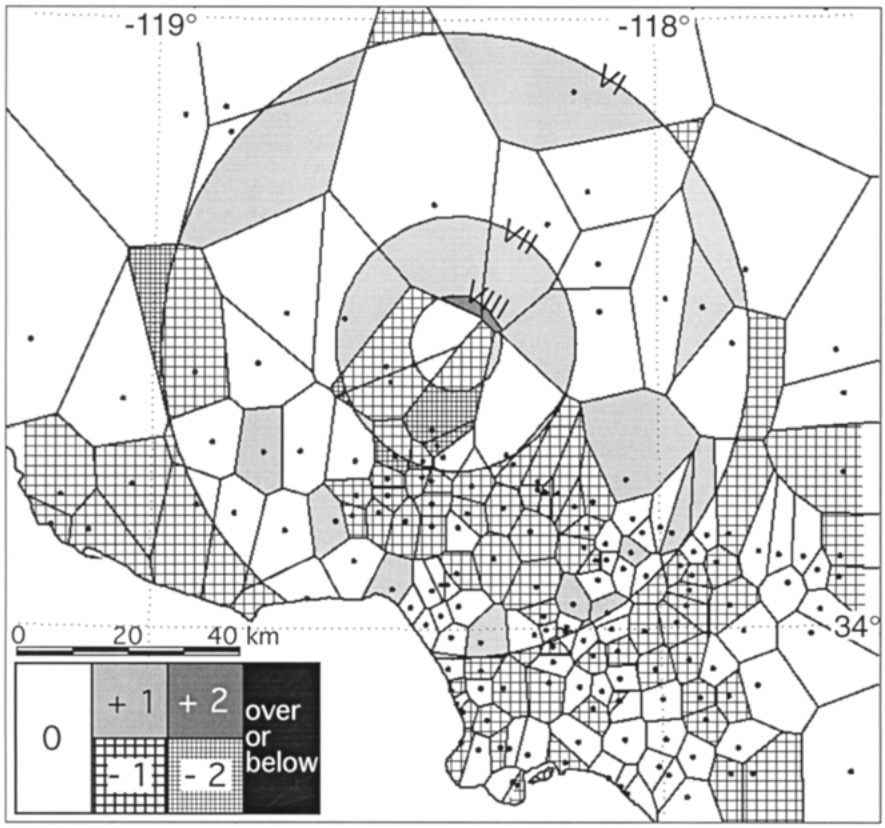

Figure 11. C-V test: pseudo-intensities forecast by the 'attenuation' relation of Figure 9, minus observations of Figure 3 (see text).

the hundreds, or thousands that provide the classification of I at a town (as in the USGS catalog). We found that these I values were independent from site characteristics in another catalogue of this kind (see the relevant analysis in Sirovich *et al.*, 1998). This could account for the ability of regional distributions of macroseismic intensities to retain traces of the source effects of some earthquakes. (Obviously, moderate and randomly distributed site effects result in an increase in noise when they are used for source retrievial).

The non-linear terms in Equation (2) accommodate, at best, the highest intensities mainly of the Northridge, San Fernando and Whittier earthquakes; including these terms in the model was a purely pragmatic choice. To overcome a similar problem, Wald *et al.* (1999; Figures 3 and 4) imposed piecewise linear regression functions to low and high levels of shaking intensities. The slightly better performance of model (2) by comparison to the previous linear regression (Sirovich *et al.*, 1998) could be, perhaps, the consequence of two circumstances: (i) the limitations of our simple source model, which approximates the unhomogeneous distribution

of energy over the real source by means of a linear source with constant energy density; and (ii) a numerical reason, i.e., the forcing of the macroseismic intensity scale on a numerical axis (the I steps perhaps shorten towards the highest degrees).

Then, it is worth discussing the nucleation used in our present and past syntheses of the San Fernando earthquake. Usually, in international literature the 'macroseismic epicenter' is informally assumed to coincide with the 'center of gravity' of the area of maximum intensity (this procedure has been recently formalized by Gasperini *et al.*, 1999). In 1996, when we back-predicted, synthetically, the isoseismals of VII and VI degree of the San Fernando earthquake (Sirovich, 1996a), our procedure pointed to an epicenter close to the 'center of gravity' of the two areas, at approximately 12–14 km south of the instrumental epicenters. Now that we invert the weighted tessellated data and the I data set from degree IX to IV, the inversion points to an epicenter close to the instrumental determinations (compare our epicenter of Figure 4, with that by Hanks, 1974, in Figure 10).

The evident discrepancy between the asymmetry in the areas of IX to VII, and the relative symmetry from VI to IV-II degrees (see Figure 3) could suggest a scattering effect and/or a double source (as in Heaton, 1982). Unfortunately, our simple model does not apply to both cases. Another inadequacy of our KF procedure is that presently we cannot simulate the rupture propagation in the dip direction. This is a serious limitation which probably made our results worse, but did not preclude the retrieval of source information from the intensity data of some other earthquakes with dip-slip mechanisms (i.e., five events in the greater Los Angeles region, and two in Nevada, Sirovich, 1996a and 1997; and the Coalinga May 2, 1983 earthquake, work in progress). Finally, given a certain rupture mechanism (and rake angle r), KF produces the same radiation adopting $r \pm 180°$, but with reversed polarities.

We emphasized the risk of using isoseismals obtained from insufficient sampling (too sparse sites) to perform inversions by trial-and-error (Pettenati *et al.*, 1999). From this point of view, Sirovich (1996a) successfully synthesized the VII and VI degree isoseismals of the San Fernando earthquake because the sampling of intensities VII and VI in the field had been more or less sufficient to allow Stover and Coffman (1993) to draw the two isolines acceptably. Thus, treating the two isoseismals qualitatively, or the observed I data set quantitatively, led to remarkable differences only in the determination of the epicenter.

Contouring based on incomplete sampling of intensity creates severe problems as, for example, in the case of the Sierra Madre earthquake of 1991 (Sirovich, 1996b). It is worth commenting, however, on the upper parts of Figures 5, 6, and 8, where sampling is scarce (few sites); consequently, rather different behaviours of the V-V and C-V tests appear there. See, for example, the upper left corners of Figures 5 and 6. The upper left polygons of Figure 5 have a residual $r = 0$; by subtracting calculation minus observation in the C-V test of Figure 6 however, one obtains high negative residuals. As said, this kind of difference could be due to the unrealistic prevalence of radiation patterns beyond approximately 60 km

from the source in our model. But there is also another argument based on the insufficient sampling there: *if* the geographical distribution of damage in 1971 had hypothetically been controlled, at least in part, by a continuous field containing high spatial frequencies, then, these high spatial frequencies would not have been revealed by the field survey. For example, in 1971 it was impossible to survey sites in the small black area of Figure 6 (just under the "−119°" label in the figure), and, thus, we consider the high residuals WNW (and ESE) of the source in Figure 6, possibly, spurious. In fact, in the C-V test, our KF output (which is continuous, and frequency-complete) is compared with discrete observations (which are frequency-incomplete, and have an unhomogeneous geographical distribution). For these reasons, our V-V test is more suitable for use as a blind test, based on experimental evidence, to judge the goodness of our fits. The C-V test helps, rather, to explain how our model works in the field.

Then, the positive and negative errors, shown in Table V, are conservative because each of them, alone, allows at least one value synthesized at a site to change by the maximum possible assumed variation (two intensity degrees).

In previous papers, we showed that our KF function is able to reproduce the gross features of the isoseismals of $\geq$VI degree of some earthquakes (Sirovich, 1996a,b, 1997). This was obtained even though our model simply considers body waves, a linear source, and an elastic homogenous half-space medium; given this medium assumption, hypocentral depth is not a crucial point, and its error less significant.

The 'attenuation' relation of Figure 9 underestimates intensity close to the epicenter (and overestimates it beyond approximately 150 km, which is out of the range of Figures 10 and 11, however). As seen, it performs relatively well in the V-V test (slightly worse than our model), but the aforementioned asymmetry of residuals in Figure 11 makes its conceptual deficiency clear. On the contrary, residuals of KF in Figure 5 are much more scattered. In other words, KF shows a greater ability of catching the physical essence of the observed phenomenon. But, from studying a greater number of earthquakes we know that KF often gives total residuals (computed independently from the distance and the azimuth) which are only slightly lower than those produced by empirical relations. Thus, to simplify matters, these relations still seem sufficient for regional hazard calculation purposes. Consider, however, that regional seismic hazard calculations use regressions obtained from *many* earthquakes occurring in *large* areas; whilst here, the starting conditions of the comparison were in favour of the 'attenuation' relation, because the one used was obtained *locally* from the data of the five earthquakes studied in the greater Los Angeles region.

Some source parameters of the San Fernando earthquake had already been successfully retrieved in a previous article, using its isoseismals of VII and VI degrees (Sirovich, 1996a). This convergence of results was possible because the isoseismals traced manually by Stover and Coffman (1993) were based on a set of control points/sites with sufficient spatial density. But this does not hold for

the higher intensities of this earthquake, and in many other cases; in fact, in this paper, as well as in other works, we showed that contouring changes the original information, leading sometimes to severe misinterpretations (Pettenati *et al.*, 1998, 1999; Cavallini *et al.*, 2000). For inversion purposes, we suggest using observations directly, or applying tessellation. Finally, consider that this paper is simply one part of a more general work which explores the quantitative treatment of atypical data, such as intensity. At this stage of our experiments, we restricted the inversions to a limited space of the parameters. In a following research we have explored the whole of the space of the angular parameters controlling the fault plane solution of the Whittier Narrows, 1987 earthquake (Pettenati and Sirovich, 2001); in that case as well the model retrieved by our inversion is not far from the ones determined instrumentally. Regarding the results of the present inversions, given the wide ranges of the explored parameters (see Section 4.1), it is highly unlikely that a model outside the adopted constraints should score lower residuals than in Table VI.

6. Concluding Remarks

It turned out that the regional intensity data set of the San Fernando, 1971 earthquake is sufficiently uncontaminated by very local site responses, and that it recorded some source effects. Thus, by inverting this data set, we retrieved kinematic characteristics of the source which are compatible with the more reliable ones obtained by other workers who treated instrumental measurements. An ambiguity of $\pm 180^\circ$ in the rake angle is unavoidable, nevertheless.

In conclusion, this paper suggests, firstly, that the representation of macroseismic intensity data can be rendered more quantitatively and objectively using the Voronoi polygons. This technique (i) honors the data completely, (ii) adds information about their spatial density and continuity, (iii) allows one to treat residuals in the azimuth-distance plane, (iv) gives an easy-to-grasp, and *reproducible* picture of damage distribution, (v) helps invert I data because it allows the treatment of residuals geographically. Secondly, it confirms that the gross geometric and kinematic source features of some earthquakes can be retrieved by inverting their observed intensities (felt reports). The complete procedure of tessellation plus inversion could allow an increase of the observation period of the seismicity in areas where good historical information is available.

It appears doubtful that our kinematic algorithm might be useful for improving regional seismic hazard calculations. But our method seems promising for treating earthquakes of the pre-instrumental era.

Acknowledgements

This research was supported by the GNDT of the Ministry of Civil Defence, and of the National Council for Research of Italy (CNR); grants 36.02963.PF54 and 37.00536.PF54. We are grateful to James W. Dewey, and to Laura Peruzza for

their valuable comments and criticisms; to David M. Boore for helpful criticisms and scientific opinions on a previous version of this paper.

References

Aki, K. and Richards, P. G.: 1980, *Quantitative Seismology, Theory and Methods*, 2 Vols., W. H. Freeman and Co., San Francisco, 932 pp.

Alewine, R. W., III: 1974, *Application of Linear Inversion Theory Toward the Estimation of Seismic Source Parameters*, Ph.D. thesis, California Institute of Technology, Pasadena, California, 303 pp.

Allen, C. R., Engen, G. R., Hanks, T. C., Nordquist, J. M., and Thatcher, W. R.: 1971, Main shock and larger aftershocks of the San Fernando earthquake, February 3 through March 1, 1971. USGS Professional paper 733 *The San Fernando, California, Earthquake of February 3, 1971*, Washington, pp. 17–20.

Bakun, W. H. and Wentworth, C. M.: 1997, Estimating earthquake location and magnitude from seismic intensity data, *Bull. Seism. Soc. Am.* **87**, 1502–1521.

Barnett V. and Lewis, T.: 1978, *Outliers in Statistical Data*, Wiley series in probability and mathematical statistics-applied, John Wiley and Sons, Chichester, 355 pp.

Bent, A. L. and Helmberger, D. V.: 1989, Source complexity of the October 1, 1987, Whittier Narrows earthquake, *J. Gephys. Res.* **34**, 3548–9556.

Bernard, P. and Madariaga, R.: 1984, A new asymptotic method for modeling of near-field accelerograms, *Bull. Seism. Soc. Am.* **74**, 539–557.

Blake, A.: 1941, On the estimation of focal depth from macroseismic data, *Bull. Seism. Soc. Am.* **31**, 225–231.

Bonilla, M. G. *et al.*: 1971, Surface faulting, *U.S. Geol. Surv. Prof. Paper* **733**, 55–76.

Boore, D. M., Joyner, W. B., Oliver III, A. A., and Page, R. A.: 1978, Estimation of Ground Motion Parameters, *Geol. Surv. Circular*, Vol. 795, U.S.G.S., Arlington, VA, 42 pp.

Cavallini, F., Bobbio, M., Pettenati, F., and Sirovich, L.: 2000, ConVor, a new-generation methodology for tracing objective and reproducible isoseismals: The case of the Feb. 28, 1925 Charlevoix earthquake in Canada, AGU Spring Meeting, Washington, May 30–June 3, 2000, *EOS, Transactions, May 9, 2000*, p. S311.

Chiaruttini, C. and Siro, L.: 1991, Focal mechanism of an earthquake of Baroque age in the 'Regno delle Due Sicilie' (southern Italy), *Tectonophysics* **193**, 195–203.

CMT catalog: 1994, in G. Ekstrom (ed.), *Centroid-Moment Tensor Catalog*, Harvard University, Cambridge, MA). Erik Larson (larson@geophysics.harvard.edu) last updated version 12/13/94.

Dengler, L. A. and Dewey, J. W.: 1998, An intensity survey of households affected by the Northridge, California, earthquake of January 17, 1994, *Bull. Seism. Soc. Am.* **88**, 441–462.

Frankel, A.: 1994, Implications of felt area-magnitude relations for earthquake scaling and the average frequency of perceptible ground motion, *Bull. Seism. Soc. Am.* **84**, 462–465.

Gasperini, P., Bernardini, F., Valensise, G., and Boschi, E.: 1999, Defining seismogenic sources from historical earthquake felt reports, *Bull. Seism. Soc. Am.* **89**, 34–110.

Hanks, T. C.: 1974, The faulting mechanism of the San Fernando earthquake, *J. Geophys. Res.* **79**, 1215–1229.

Hanks, T. C. and H. Kanamori, 1979, A moment-magnitude scale, *J. Geophis. Res.* **84**, 2348–2350.

Heaton, T. H.: 1982, The 1971 S. Fernando earthquake: A double event?, *Bull. Seism. Soc. Am.* **72**, 2037–2062.

Jànosi, J. V.: 1907, Makroszeizmikus rengések feldolgozàsa a çancani-féle egyenlet alapjàn, *Az 1906 èvi Magyarorszàgi földrengèsek*, 77–88.

Johnston, A. C.: 1996a, Seismic moment assessment of earthquakes in stable continental regions – I. Instrumental seismicity, *Geophys. J. Int.* **124**, 381–414.

Johnston, A. C.: 1996b, Seismic moment assessment of earthquakes in stable continental regions – II. Historical seismicity, *Geophys. J. Int.* **125**, 639–678.

Kamb, B., Silver, L. T., Abrams, M. J., Carter, B. A., Jordan, T. H., and Minster, J. B.: 1971, Pattern of faulting and nature of fault movement in the San Fernando earthquake, USGS Professional paper 733 *The San Fernando, California, Earthquake of February 3, 1971*. Washington, pp. 41–54.

von Kövesligethy, R.: 1907, Seismischer Stärkegrad und Intensität der Beben, *Gerlands Beitr. Geophysik* **8**, 363–366.

Langston, C. A.: 1978, The February 3, 1971, San Fernando earthquake: A study of source finiteness in teleseismic body waves, *Bull. Seism. Soc. Am.* **68**, 1–29.

Li, X. and Götze, H.-J.: 1999, Comparison of some gridding methods, *The Lead. Edge* **8**, 898–900.

Ma, K-F. and Kanamori, H.: 1994, Broadband waveform observation of the 28 June 1991 Sierra Madre earthquake sequence (ML = 5.8), *Bull. Seism. Soc. Am.* **84**, 1725–1738.

Madariaga, R. and Bernard, P.: 1985, Ray theoretical strong motion synthesis, *J. Geophys.* **58**, 73–81.

Mallet, R.: 1862, *The Great Neapolitan Earthquake of 1857*, 2 Vols., Chapman and Hall, London, pp. 431, 399.

Ohta, Y. and Satoh, K.: 1980, Analyses on seismic intensity and earthquake disaster in the Caldiran earthquake, in Y. Ohta (ed.), *Engineering Seismological Studies on the 24 November 1976 Caldiran Earthquake in Turkey*, Dept. Arch. Eng., Hokkaido University, Sapporo, pp. 89–117.

Panza, G. F., Craglietto, A., and Suhadolc, P.: 1991, Source geometry of historical events retrieved by synthetic isoseismals, *Tectonophysics* **193**, 173–184.

Pettenati, F., Cavallini, F., and Sirovich, L.: 1998, Quantitative treatment of macroseismic intensity and objective evaluation of synthetic results, in Philippe Bisch, Pierre Labb, and Alain Pecker (eds.), *Proc. 11th Europ. Conf. on Earthq. Engng.*, Paris, Sep. 6–11, 1998. Balkema, Rotterdam, CD-ROM (p. 10; file PETQTO.PDF).

Pettenati, F., Sirovich, L., and Cavallini, F.: 1999, Objective treatment, and synthesis of macroseismic intensity data sets using tessellation, *Bull. Seism. Soc. Am.* **89**, 1203–1213.

Pettenati, F. and Sirovich, L.: 2001, New-generation objective and reproducible isoseismals, and tests of source inversion of the Usgs "Felt Reports", *Proc. 4th Int. Conf. on Rec. Adv. Geotech. Earthq. Engng. & Soil Dyn.*, San Diego, CA, March 26–31, 2001, University of Missouri-Rolla, in press on CD-ROM.

Preparata, F. P. and Shamos, M. I.: 1985, *Computational Geometry: An Introduction*, Springer Verlag, New York, pp. 390, 398.

Press, W. H., Teukolsky, S. A., Vetterling, W. T., and Flannery, B. P.: 1994, *Numerical Recipes*, 2nd edn, Cambridge University Press, New York, 963 pp.

Sachs, L.: 1984, *Applied Statistics: A Hand Book of Technique*, 2nd edn, Springer Series in Statistics, Springer Verlag, New York, 707 pp.

Sambridge, M., Braun, J., and McQueen, H.: 1995, Geophysical parametrization and interpolation of irregular data using natural neighbours, *Geophys. J. Int.* **122**, 837–857.

Scholz, C. H.: 1971, Microearthquakes on the San Andreas fault and aftershocks of the San Fernando earthquake, USGS Professional paper 733 *The San Fernando, California, Earthquake of February 3, 1971*, Washington, pp. 33–37.

Shebalin, N. V.: 1973, Macroseismic data as information on source parameters of large earthquakes, *Phys. Earth Planet. Interiors* **6**, 316–323.

Sirovich, L.: 1996a, A simple algorithm for tracing out synthetic isoseismals, *Bull. Seism. Soc. Am.* **86**, 1019–1027.

Sirovich, L.: 1996b, Synthetic isoseismals of two Californian earthquakes, *Nat. Hazards 14*, 23–37.

Sirovich, L.: 1997, Synthetic isoseismals of three earthquakes in California-Nevada, *Soil Dyn. and Earthq. Engng.* **16**, 353–362.

Sirovich, L, Pettenati, F., and Bobbio, M.: 1998, Site effects of an M = 7.1–7.5 earthquake, and its tessellated synthesis, *Proc. 11th Danube-European Conf. on Soil Mech. and Found. Engng.*, Porec, May 25–29, 1998, Balkema, Rotterdam, pp. 349–358.

Song, X. J., Jones, L. E., and Helmberger, D. V.: 1995, Source characteristics of the 17 January 1994 Northridge, California, earthquake from regional broadbend modeling, *Bull. Seism. Soc. Am.* **85**, 1591–1603.

Sponheuer, W.: 1960, Berechnungsverfahren mit schrittweiser Näherung, in W. Sponheuer (ed.), *Methoden zur Herdtiefen Bestimmung in der Makroseismik*, Freiberger Forschungshefte C88, Akademie Verlag, Berlin, pp. 16–32.

Spudich, P. and Frazer, L. N.: 1984, Use of ray theory to calculate high-frequency radiation from earthquake sources having spatially variable rupture velocity and stress drop, *Bull. Seism. Soc. Am.* **74**, 2061–2082.

Stover, C. W. and Coffman, J. L. (eds.): 1993, *Seismicity of the United States, 1568–1989 (Revised)*, U.S. Geol. Survey Prof. Paper 1527, Washington.

Suhadolc, P., Cernobori, L., Pazzi, G., and Panza, G. F.: 1988, Synthetic isoseismals, in J. Bonnin, M. Cara, A. Cisternas, and R. Fantechi (eds.), *Seismic Hazard in Mediterranean Regions*, Kluwer, Dordrecht, pp. 205–228.

U.S. Geological Survey Staff: 1971, Surface faulting, USGS Professional paper 733, *The San Fernando, California, Earthquake of February 3, 1971*. Washington, pp. 55–76.

Wald, D. J., Quitoriano, V., Heaton, T. H., and Kanamori, H.: 1999, Relationships between peak ground acceleration, peak ground velocity and modified Mercalli intensity in California, *Earthquake Spectra* **15**, 557–564.

Whitcomb, J. H.: 1971, Fault-plane solutions of the February 3, 1971, San Fernando earthquake and some aftershocks. USGS Professional paper 733, *The San Fernando, California, Earthquake of February 3, 1971*, Washington, pp. 30–32.

Whitcomb, J. H., Allen, C. R., Garmany J. D., and Hileman, J. A.: 1973, San Fernando earthquake series, 1971: Focal mechanisms and tectonics, *Rev. Geophys. Space Phys.* **11**, 693–730.

Wood, H. O. and Neumann, F.: 1931, Modified Mercalli intensity scale of 1931, *Bull. Seism. Soc. Am.* **21**, 277–283.

Zahradnik, J.: 1989, Simple method for combined studies of macroseismic intensities and focal mechanisms, *Pure Appl. Geophys.* **130**, 83–97.